Probabilistic Optimal Power Flow in Large-Scale Electric Transmission Systems through a Matheuristic Solution Approach

Wmerson Claro de Oliveira, Jairo Gonzalo Yumbla Romero, Lucas do Carmo Yamaguti, Juan M. Home-Ortiz, and José Roberto Sanches Mantovani, *Member, IEEE*

***Abstract*— This paper proposes a new optimization methodology to solve the AC optimal power flow (OPF) problem considering renewable energy sources (RES). The formulation of the OPF problem comprises the minimization of power generation costs and gas emissions considering a set of operational and physical constraints. This minimization is achieved through controlling power dispatch generators, position changing of the tap transformers, and controllable reactive shunt compensation. RES and demand uncertainties are modeled using the (2m+1) point-estimate method. The mathematical formulation of the OPF problem is a mixed-integer nonlinear programming multiobjective model. A matheuristic algorithm is proposed to solve this problem efficiently, combining a classic nonlinear OPF model and the Variable Neighborhood Descent (VND) metaheuristic algorithm. The potential of the proposed algorithm is shown through numerical experiments carried out using the IEEE 300-bus systems.**

***Index Terms*— Matheuristic, multiobjective optimization, probabilistic optimal power flow, VND heuristic approach**

NOMENCLATURE

Sets and indices

i, j	Index for buses
ij	Index for transmission lines
s	Index for stochastic scenarios
Γ_B	Set of buses
Γ_{SH}	Set of buses with a controllable capacitive reactive power source (shunt compensator)
Γ_L	Set of transmission lines
Γ_S	Set of load scenarios
Γ_G	Set of generation buses (thermal)
Γ_R	Set of generation buses with renewable energy sources (wind and photovoltaic)
Γ_T	Set of lines with a transformer with automatic tap control

Parameters

a_i, b_i, c_i	Cost coefficients for active power generation
$\gamma_i, \beta_i, \alpha_i, \xi_i, \lambda_i$	Emission coefficients for active power generation in thermal generators
b_{ij}^{sh}	Shunt susceptance of the branch
g_i^{sh}, b_i^{sh}	Shunt conductance and susceptance
g_{ij}, b_{ij}	Series conductance and susceptance
h_s	Number of hours in load scenario s
φ_{ij}	Angle variation of the phase-shifting transformer at line ij
k_{tp}, k_{sh}	Number of changed positions on taps of the OLTCs and controllable shunt compensators, respectively
$\overline{n}_i^{sh}$	Maximum number of shunt compensator modules
$\overline{n}_{ij}^{t}$	Maximum number of tap positions of transformers
$\ddot{n}_{ij,s}^{t}$	Current position of the tap of the OLTC at line ij
$\ddot{n}_{ij,s}^{sh}$	Current position of the shunt compensator at bus i
r_{ij}	Voltage regulation ratio of transformer at line ij
$\overline{S}_{ij}$	Maximum apparent power flow
$\underline{v}_i, \overline{v}_i$	Minimum and maximum voltage magnitude limits
$P_{i,s}^{D}, Q_{i,s}^{D}$	Active and reactive power demands
$\underline{P}_i^T, \overline{P}_i^T$	Minimum and maximum active power generation capacities (thermal generation)
$\underline{P}_{i,s}^{W/PV}, \overline{P}_{i,s}^{W/PV}$	Minimum and maximum active power generation capacities (wind turbine and solar panel generation)
$\underline{Q}_i^T, \overline{Q}_i^T$	Minimum and maximum reactive power generation capacities (thermal generation)
$\underline{Q}_{i,s}^{W}, \overline{Q}_{i,s}^{W}$	Minimum and maximum reactive power generation capacities (wind turbine)
ρ	Penalty parameter
$\underline{\theta}_{ij}, \overline{\theta}_{ij}$	Minimum and maximum allowed difference of voltage angle between buses ij
ω	Weight parameter for the objective function
$\Delta\omega$	Weight steps

Continuous variables

$a_{ij,s}$	Transformation ratio 1: t of the transformer installed at line ij
$P_{i,s}^{T/W}, Q_{i,s}^{T/W}$	Active and reactive power generation (thermal generator and wind turbine)
$P_{i,s}^{PV}$	Active power generation (photovoltaic generator)
$\tilde{P}_{i,s}, \tilde{Q}_{i,s}^{c}, \tilde{Q}_{i,s}^{i}$	Penalization variable for active, capacitive, and inductive power, respectively
$p_{ij,s}, q_{ij,s}$	Active and reactive power flow at line ij
$v_{i,s}$	Voltage magnitude at bus i
$w_{i,s}$	An auxiliary variable that determines the percentage capacity of the shunt compensator connected at bus i. (value between 0 and 1)
$\theta_{ij,s}$	Voltage angle difference between buses ij

Discrete variables

$n_{i,s}^{sh}$	Number of switches for automatic reactive control of the shunt compensator
$n_{ij,s}^{t}$	Position of transformer taps at line ij

This work was supported by the São Paulo Research Foundation (FAPESP) under grants 2019/01841-5, 2019/23755-3 and 2015/21972-6, the Coordination for the Improvement of Higher Education Personnel (CAPES) finance code 001, and the Brazilian National Council for Scientific and Technological Development (CNPq) under grants 164751/2018-1 and 304726/2020-6.

Wmerson Claro de Oliveira, Jairo Gonzalo Yumbla Romero, Lucas do Carmo Yamaguti, Juan M. Home-Ortiz and José Roberto Sanches Mantovani are with the Department of Electrical Engineering, Power System Planning Lab, Sao Paulo State University (UNESP), Ilha Solteira–SP, Brazil (e-mails: wmerson14webing@gmail.com, jairo.yumbla@unesp.br, lucas.yamaguti@unesp.br, juan.home@unesp.br, mant@dee.feis.unesp.br)

I. INTRODUCTION

The AC optimal power flow (OPF) is a generic denomination of a classic and fundamental computational tool used to

analyze the operation and planning of electric power systems. The formulation of the OPF problem is a mixed-integer nonlinear programming (MINLP) model that aims to obtain the adjustments of control variables (integer and continuous) to determine the optimal operating state of an electric power system, taking into account a set of physical and operational constraints of installed devices and transmission network. The OPF is an NP-hard, multi-modal, and non-convex problem that is highly difficult to solve because of the large number of variables, objectives, and constraints in the optimization process [1]–[3]. Also, in the OPF model, different objectives can be considered, individual or simultaneous (for example, dispatch of active and reactive powers, reduction of operating costs, environmental objectives, etc.). In this way, new modeling approaches and specialized solution techniques are required to deal with these problems.

Global awareness concerning environmental preservation guides studies toward new research fields. The focus is on developing projects and operational strategies that aim to reduce the emission of polluting gases from the energy generation of thermoelectric plants [4]–[8]. In this sense, planners are challenged to solve the problem of environmental/economic dispatch (EED) to find an optimal operating state considering the simultaneous optimization of generation costs and pollutant gas emissions [9]–[11]. Therefore, this problem can be modeled as a multiobjective optimization problem with two or more conflicting objectives.

In the literature, several works propose changes in operating strategies of power systems, aiming to mitigate the environmental impact with minimum generating costs. In this regard, multiobjective approaches to minimize the generation costs and greenhouse gas (GHG) emission mitigation can be found in [12]–[16]. In [12], a nondominated sorting genetic algorithm (NSGA) is used to solve the nonlinear and constrained EED problem. The proposed NSGA preserves the diversity of the population to avoid problems of premature convergence to generate a set of nondominated solutions that are not distributed in the Pareto frontier. This method was tested using a small-scale test system. In [13], a multiobjective particle swarm optimization (PSO) is proposed to solve the EED problem. The authors in [14] propose a multiobjective differential evolution algorithm to solve the EED problem formulated as a nonlinear constrained model with three conflicting objectives: power generation fuel cost, GHG emission mitigation, and power losses. In reference [15] it is proposed a nonlinear fractional programming approach that considers two simultaneous nonlinear programming (NLP) models to optimize the generating cost and the total GHG emissions. In [16], the main objectives are the generation costs and emission mitigation; a multiobjective harmony search algorithm that uses a non-dominated solution strategy to propose a Pareto-optimal set of results is used to deal with the problem. The formulations in [12]–[16] do not consider that renewable generation sources are installed in the system.

Several meta-heuristic algorithms that minimize the fuel generating cost and the emission mitigation combined into a single objective function can be found in the literature [17]–[23]. In [17], an artificial bee colony algorithm with local search is used to solve the EED problem. In [18], a multiobjective backtracking search algorithm is proposed. In [19], the conflicting objectives of the EED problem are combined in a fuzzy framework by suggesting adjusted fuzzy membership functions; then, a PSO algorithm is used to solve the problem. In [20], a flower pollination algorithm is used for the problem. In [21] and [22], the authors propose a hybrid firefly algorithm and bat algorithm to solve the EED. In [23], the EED problem is solved via a meta-heuristic algorithm inspired by kernel tricks. The EED problem can also consider specific characteristics of the power systems [24], [25]. In [24], a multiobjective harmony search algorithm is used to solve an EED problem considering the minimization of the power losses of the electric network. In [25], a hybrid PSO and gravitational search algorithm are proposed to solve the EED problem considering multiple fuels of generation units, prohibitive operating zones for generating units, valve-point effects, and power losses. In [17]–[25], the emission reduction is considered only by optimal power dispatch of thermal power generating units while the renewable energy sources (RES) (wind and photovoltaic power generations) are disregarded. Similarly, these papers do not consider the optimal operation of control devices such as shunt compensators and automatic tap control of transformers.

Metaheuristic algorithms are presented in [26]–[28] to solve the EED considering hydro, thermal, and wind power units. In [26], a method that combines the modified quantum-behavior lightning search algorithm and artificial intelligence technique is used. In [27], a modified PSO algorithm is used to solve the problem considering an hour-by-hour power dispatch. The authors in [28] also consider photovoltaic generation, and the optimization model is solved via a multiobjective hybrid grey wolf optimizer algorithm. It is worth mentioning that works [26]–[28] disregarded the optimization of the voltage control devices.

According to literature, the EED has been approached from the optimal power dispatch where voltage control devices have not been adequately considered. Usually, these devices require integer variables to be included in the EED's mathematical model, which increases the problem complexity [29]. Therefore, the authors in [29] propose a multiobjective probabilistic AC-OPF model for medium-term electrical power systems operation with high RES penetration. An NSGA-II algorithm is used to solve it, while uncertainties are considered through the point-estimate method. The optimization model also considers the voltage control devices with the optimization of the shunt compensators and the tap position of the transformers. In relation to [29], our paper proposes a new technique to solve the problem of OPF formulated as a stochastic mixed integer nonlinear programming model through an implicit decomposition scheme called matheuristic. In reference [31], the solution technique proposed is a matheuristic approach similar to the proposal in this paper to solve a deterministic single-objective MINLP model for large-size systems. However, reference [31] does not include RES or demand behavior uncertainties.

This work proposes a new specialized matheuristic optimization technique to solve the AC-OPF problem minimizing the generation costs and greenhouse gas emissions. The proposed approach uses classical optimization to solve the continuous variables of the problem, while a neighborhood search heuristic algorithm is used to manage the search space of the integer variables. The mathematical model considers the optimal dispatch of active and reactive powers of wind turbines and non-renewable generators, the active power dispatch of photovoltaic units, and the adjustment of the voltage control devices. Furthermore, the proposed approach uses the (2m+1) point-estimate method to deal with uncertainties on demand and RES (wind and photovoltaic). The AC-OPF formulation is a multiobjective MINLP model that, due to the multi-modal and non-convexity characteristic, is difficult to solve through classical optimization techniques. According to the presented state of the art, the contributions of this paper are the follows:

- Reformulate the multiobjective MINLP stochastic model to solve the environmental/economic AC-OPF problem for large-scale transmission systems, considering the uncertainty behavior of the RES (wind and photovoltaic generation) and loads. The discrete variables of the model represent the taps position of transformers and shunt compensators.
- Reformulate based on the proposals of [31] the specialized hybrid matheuristic approach (MA) based on the variable neighborhood descend (VND) heuristic to solve the environmental/economic AC-OPF stochastic model for large-scale electric power transmission systems.
- A new and efficient set of neighborhood structures are proposed for the AC-OPF problem. These structures are a novel view for optimizing power systems that can be applied to other problems.

The remainder of this paper is organized as follows: Section II presents the problem formulation of the environmental/economic AC-OPF as an MINLP model. Section III presents the proposed matheuristic approach; the principal remarks of the (2m+1) point-estimate method are also provided. Sections IV and V present the results and discussions of the simulations performed, respectively. Finally, relevant conclusions are drawn in Section VI.

II. Mathematical Model

In this section, the AC-OPF problem is modeled as a deterministic multiobjective MINLP problem in which the objective functions represent the minimization of the generation cost and the GHG emissions, subject to the physical and operational constraints of the electrical power system. Integer variables determine the operation of the shunt compensators and on-load tap changer transformers (OLTC). The formulation includes thermal generation, RES (wind and photovoltaic generation), and load scenarios. The mathematical model of the problem is presented in the set of equations (1)-(19).

$$f^A = \sum_{s\in\Gamma_s} h_s \sum_{i\in\Gamma_G} \left(a_i\left(P_{i,s}^T\right)^2 + b_i P_{i,s}^T + c_i\right) \quad (1)$$

$$f^B = \sum_{s\in\Gamma_s} h_s \sum_{i\in\Gamma_G} \left[10^{-2}\left(\gamma_i\left(P_{i,s}^T\right)^2 + \beta_i P_{i,s}^T + \alpha_i\right) + \xi_i exp\left(\lambda_i P_{i,s}^T\right)\right] \quad (2)$$

Subject to:

$$P_{i,s}^T + P_{i,s}^W + P_{i,s}^{PV} + \tilde{P}_{i,s} - P_{i,s}^D - g_i^{sh} v_{i,s}^2 - \sum_{ij\in\Gamma_L} p_{ij,s} - \sum_{ji\in\Gamma_L} p_{ji,s} = 0 \quad (3)$$

$$Q_{i,s}^T + Q_{i,s}^W + \tilde{Q}_{i,s}^c - \tilde{Q}_{i,s}^i - Q_{i,s}^D + b_i^{sh} v_{i,s}^2 w_{i,s} - \sum_{ij\in\Gamma_L} q_{ij,s} - \sum_{ji\in\Gamma_L} q_{ji,s} = 0 \quad \forall(i\in\Gamma_B, s\in\Gamma_S) \quad (4)$$

$$p_{ij,s} = (a_{ij,s}v_{i,s})^2 g_{ij} - \left(a_{ij,s}v_{i,s}\right)v_{j,s}[g_{ij}cos(\theta_{ij,s}+\varphi_{ij}) + b_{ij}sen(\theta_{ij,s}+\varphi_{ij})] \quad (5)$$

$$p_{ji,s} = {v_{j,s}}^2 g_{ij} - \left(a_{ij,s}v_{i,s}\right)v_{j,s}[g_{ij}cos(\theta_{ij,s}+\varphi_{ij}) - b_{ij}sen(\theta_{ij,s}+\varphi_{ij})] \quad (6)$$

$$q_{ij,s} = -\left(a_{ij,s}v_{i,s}\right)^2\left(b_{ij}+\frac{b_{ij}^{sh}}{2}\right) + \left(a_{ij,s}v_{i,s}\right)v_{j,s}[b_{ij}cos(\theta_{ij,s}+\varphi_{ij}) - g_{ij}sen(\theta_{ij,s}+\varphi_{ij})] \quad (7)$$

$$q_{ji,s} = -{v_{j,s}}^2\left(b_{ij}+\frac{b_{ij}^{sh}}{2}\right) + \left(a_{ij,s}v_{i,s}\right)v_{j,s}[b_{ij}cos(\theta_{ij,s}+\varphi_{ij}) + g_{ij}sen(\theta_{ij,s}+\varphi_{ij})] \quad \forall(ij\in\Gamma_L, s\in\Gamma_S) \quad (8)$$

$$w_{i,s} = \left(\frac{n_{i,s}^s}{\overline{n}_i^s}\right) \quad \forall(i\in\Gamma_{SH}, s\in\Gamma_S) \quad (9)$$

$$a_{ij,s} = 1 + \left(\frac{n_{ij,s}^t r_{ij}}{\overline{n}_{ij}^t}\right) \quad \forall(ij\in\Gamma_T, s\in\Gamma_S) \quad (10)$$

$$\underline{v}_i \le v_{i,s} \le \overline{v}_i \quad \forall(i\in\Gamma_B, s\in\Gamma_S) \quad (11)$$

$$\underline{P}_i^T \le P_{i,s}^T \le \bar{P}_i^T \quad \forall(i\in\Gamma_G, s\in\Gamma_S) \quad (12)$$

$$\underline{P}_{i,s}^{W/PV} \le P_{i,s}^{W/PV} \le \bar{P}_{i,s}^{W/PV} \quad \forall(i\in\Gamma_R, s\in\Gamma_S) \quad (13)$$

$$\underline{Q}_i^T \le Q_{i,s}^T \le \bar{Q}_i^T \quad \forall(i\in\Gamma_G, s\in\Gamma_S) \quad (14)$$

$$\underline{Q}_{i,s}^W \le Q_{i,s}^W \le \bar{Q}_{i,s}^W \quad \forall(i\in\Gamma_R, s\in\Gamma_S) \quad (15)$$

$$(p_{ij,s})^2 + (q_{ij,s})^2 \le \left(\overline{S}_{ij}\right)^2 \quad \forall(ij\in\Gamma_L, s\in\Gamma_S) \quad (16)$$

$$\underline{\theta}_{ij} \le \theta_{ij,s} \le \overline{\theta}_{ij} \quad \forall(ij\in\Gamma_L, s\in\Gamma_S) \quad (17)$$

$$0 \le n_{i,s}^{sh} \le \overline{n}_i^{sh} \quad \forall(i\in\Gamma_{SH}, s\in\Gamma_S) \quad (18)$$

$$-\overline{n}^t{}_{ij} \le n_{ij,s}^t \le \overline{n}^t{}_{ij} \quad \forall(ij\in\Gamma_T, s\in\Gamma_S) \quad (19)$$

In (1), the objective function f^A determines the generation cost of generating units, and according to the adequate specification of coefficients a_i, b_i and c_i it is possible to model thermal, hydraulic, photovoltaic, and wind generators. In (2), the objective function f^B models the GHG emissions such as Sulphur oxides SO_x and Nitrogen oxides NO_x [5]. Constraints (3) and (4) represent the active and reactive power flow balances, respectively, while (5)-(8) determine the calculation of the flow of active and reactive power through the lines. Constraints (9) and (10) determine the percentage reactive power injection of the shunt compensators and the OLTC ratio, respectively. Constraint (11) represents the operational limits of the voltage magnitude in the system buses. The active and reactive power generation limits for thermal, wind turbines and photovoltaic generation are presented in (12)-(15), respectively. Constraint (16) is incorporated into the model to express the

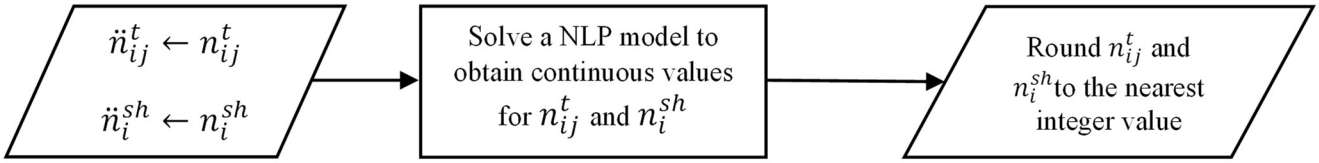

Fig. 1. Proposed basic neighborhood structures.

thermal limit of transmission lines. The limits of the angle differences between buses are modeled in (17). The limits of capacitive/reactive variables and taps of OLTCs are modeled in (18) and (19), respectively.

A. RESs Models

The available power of PV units and wind turbines, by scenario, are presented in (20) and (21), respectively.

$$\bar{P}_{i,s}^{PV} = \bar{P}_{i}^{PV}\left(\frac{G_s}{1000}\left[1+\delta((T_b+\left(\frac{NOCT-20}{800}\right)I_s)-25)\right]\right) \tag{20}$$

Where $\bar{P}_i^{PV}$ is the active output power of the PV unit at node i under normal operational conditions, G_s is the solar irradiance in scenario s, δ is a power temperature constant, T_b is the ambient temperature, and $NOCT$ is the nominal operating cell temperature.

$$\bar{P}_{i,s}^{W} = \begin{cases} 0, & v_s < v_0 \\ \dfrac{\bar{P}_i^W}{v_r - v_0} v_s + \bar{P}_i^W\left(1 - \dfrac{v_r}{v_r - v_0}\right) & v_0 \le v_s < v_r \\ \bar{P}_i^W & v_r \le v_s < v_m \\ 0 \quad v_s \ge v_m \end{cases} \tag{21}$$

Where $\bar{P}_i^W$ is the rated active output power of the wind turbine installed at node i, v_s is the wind speed in scenario s, parameters v_0, v_r, and v_m represent the cut-in wind speed, rated wind speed, and cut-out wind speed, respectively.

B. Reformulation of the OPF Mathematical Model

Metaheuristics algorithms allow infeasible solutions during the optimization process and explore the search space even though a set of infeasible solutions. In the OPF problem, the infeasibility can be controlled by adding the positive penalization variables $\tilde{P}_{i,s}$, $\tilde{Q}_{i,s}^{c}$, and $\tilde{Q}_{i,s}^{i}$ in the active and reactive power balance constraints (3) and (4). In order to assess the quality of the solutions during the optimization process, the penalization variables are penalized according to the function f^P, presented in (22).

$$f^P = \sum_{s\in\Omega_s} h_s\left(\left(\tilde{P}_{i,s}\right)^2 + \left(\tilde{Q}_{i,s}^{c}\right)^2 + \left(\tilde{Q}_{i,s}^{i}\right)^2\right)\rho \tag{22}$$

The AC-OPF multiobjective model (1)–(19) is reformulated as a single-objective problem through the weighted sum method plus a penalty function (f^P), according to (23). This approach evaluates several alternatives in terms of the combination of objectives, f^A and f^B, considering the parameter $\omega \in [0-1]$. In this case, ω determines the level of importance that the decision maker attributes to each objective.

$$min\ f = (\omega)f^A + (1-\omega)f^B + f^P \tag{23}$$

III. Solution Technique

Establishing a solution technique to find high-quality solutions for large-scale and complex optimization problems is challenging. Although it is possible to formulate an explicit mathematical model, in many cases, modern optimization solvers may fail to solve such problems. In this way, the MINLP model (1)–(23) is a non-convex problem that cannot solve directly using classical optimization techniques for large power systems. This section presents a matheuristic approach that uses NLP optimization models and the structure of the VND meta-heuristic algorithm to solve the multiobjective MINLP model (1)–(21), determining a set of Pareto solutions with the optimal value of the integer and continuous variables of the problem [31]. Besides, the principal remarks of the (2m+1) point-estimate method are provided.

A. Probabilistic Optimal Power Flow (POPF)

The behavior of the power system is subject to uncertainties; thus, probabilistic approaches are necessary to determine the operating state of the systems under uncertainties [32]–[35]. In this paper, we use the concepts of Hong's point estimate method (2m+1) [36] to solve the probabilistic OPF (POPF), incorporating uncertainties in the RESs (wind speed and solar irradiance) and load. In comparison with the (2m+1) POPF proposed in [34], where a deterministic power flow is used to determine the moment functions, in this paper, these concentrations values are determined by a deterministic AC-OPF, i.e., by the solution of the optimization model (1)–(21) via optimization solver. It is worth mentioning that the on-load tap changer (OLTC) of transformers and shunt compensators are input parameters of the POPF, so these variables are not optimized at this point. However, the optimization of these variables is carryout by the proposed matheuristic algorithm, presented in the following subsection.

B. Matheuristic Approach

Matheuristics are sturdy optimization techniques that combine heuristics algorithms and classical mathematical programming to solve specific large and complex optimization problems [38]. In general, the matheuristic optimization techniques take advantage of the exact methods' optimality and the speed of heuristics. This interoperation recently has shown high efficiency and scalability in solving problems related to electric power systems. Moreover, matheuristic techniques have well managed the high combinatorial complexity linked to these problems.

In this work, the matheuristic concept was implemented using a VND heuristic algorithm and an MINLP model (1)-

(23) to determine the optimal value of variables. The VND is the most simplified version of the Variable Neighborhood Search algorithms and is based on repetitive local optimization through different search spaces. An essential feature of these algorithms is that, during the process, it uses different neighborhood structures to explore high-quality solutions and move forward. Generally, a VND algorithm is a deterministic process that starts from an initial solution x and looks for a pronounced descent direction within a variable neighborhood. In summary, the process optimizes several simple and computationally light models in different search spaces, obtaining an optimization of the complete MINLP model [31]. Different from [31], this work analyzes the solution method developed in classic and large-size systems through a probabilistic approach that deals with integer and discrete variables and the uncertainties of RES and demand behavior.

The most significant interest of the algorithm is focused on the integer variables, which increase the complexity of the problem and, therefore, must be handled in a schematic way. Due to this, the neighborhood structures proposed in the following sections manage NLP models derived from MINLP (1)– (*23*) in order to determine a good value for the integer variables. The several NLP models (neighborhoods) are treated via an optimization solver to obtain an optimal solution for the respective neighborhood. The algorithm is repeated if the stop criterion is not met. When the process stops, it is because it has not been possible to improve the solution during several iterations.

1) Initial Solution:

The initial solution of the algorithm is obtained through a nonlinear AC-OPF deterministic model, which is obtained by relaxing the integrality of the discrete variables related to the taps of OLTC ($n_{ij,s}^{t}$) and shunt reactive compensators ($n_{i,s}^{sh}$). For all the load scenarios s, only mean values of load, wind speed, and solar irradiation are considered. The obtained relaxed model is solved using a nonlinear solver, and the obtained values for $n_{ij,s}^{t}$ and $n_{i,s}^{sh}$ are rounded to the nearest discrete value.

2) Neighborhood Structures:

In the execution of the VND matheuristic algorithm, three criteria are used to define the neighborhood structures. They all manage the integer variables related to OLTCs and shunt compensators and follow the scheme shown in Fig. 1. The parameter $\ddot{n}^{t}$ is updated with the current value of each OLTC tap position while $\ddot{n}^{sh}$ takes the current state of modules at each shunt compensator. These parameters are used in the constraints of simplified NLP models that consider the relaxation of the integer variables ($n_{ij}^{t}; n_{i}^{sh} \in [0,1]$). Finally, the scheme performs a round of n_{ij}^{t} and n_{i}^{sh} to their nearest integer value.

Neighborhood Structure N_1

Structure N_1 aims to look for a better-quality neighbor, varying the values of variables $n_{ij,s}^{t}$ and $n_{i,s}^{sh}$ provided by the algorithm illustrated in Fig. 1. This structure solves a modified and relaxed deterministic AC-OPF model that is obtained through average values of the uncertain parameters. The modified model adds the constraints (24) and (25) to the complete (1)-(19) model, where (24) allows the modification of the current position of each OLTC's taps in $\pm k_{tp}$ steps. On the other hand, constraint (25) allows the modification in the current active modules of each shunt compensator in $\pm k_{sh}$ steps.

$$\ddot{n}_{ij,s}^{t} - k_{tp} \le n_{ij,s}^{t} \le \ddot{n}_{ij,s,c}^{t} + k_{tp} \qquad \forall (ij \in \Gamma_T, s \in \Gamma_S) \tag{24}$$

$$\ddot{n}_{i,s}^{sh*} - k_{sh} \le n_{i,s}^{sh} \le \ddot{n}_{i,s}^{sh} + k_{sh} \qquad \forall (i \in \Gamma_{SH}, s \in \Gamma_S) \tag{25}$$

The solution of the modified model provides a continuous solution for $n_{ij,s}^{t}$ and $n_{i,s}^{sh}$ then, this solution is rounded to the nearest discrete value. For example, if $k_{tp} = k_{sh} = 1$, this neighborhood structure allows an increase or decrease in the current values of all $n_{ij,s}^{t}$ and $n_{i,s}^{sh}$ in one position from their current states $\ddot{n}_{ij,s}^{t}$ and $\ddot{n}_{i,s}^{sh}$, respectively. This condition does not require modification of all taps of OLTCs or modules state of shunt compensators, so it is possible to maintain the current position of some or all these variables to preserve the optimality of the solution.

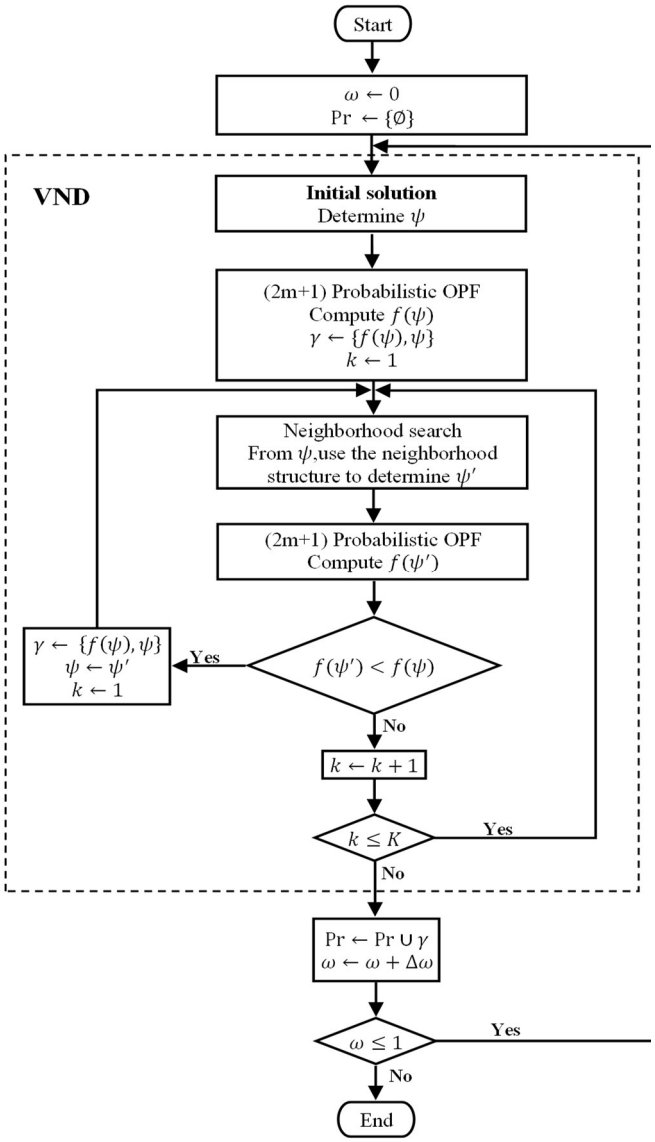

Fig. 2. Proposed MA for the multi-objective POPF

TABLE I
WIND AND PHOTOVOLTAIC GENERATIONS PROBABILISTIC PARAMETERS

Scenario (s)	Time (h_s)	Load (%)		Wind Generation (m/s)		Photovoltaic Generation (W/m²)	
		μ_s	σ_s	μ_W	σ_W	μ_{PV}	σ_{PV}
1	2000	50	10	7.72	4.45	0.00	0.00
2	5760	80	11	8.09	4.24	650	300
3	1000	100	12	8.48	3.61	0.00	0.00

TABLE II
TYPES OF GENERATION UNITS INSTALLED IN THE SYSTEM FOR CASE 2

Type	Capacity installed (%)	Bus						
Thermal	46.38	20	76	84	92	98	124	141
		147	149	171	190	198	220	221
		222	227	236	239	241	243	7003
		7011	7012	7039	7057	7061	7062	7130
		7139	7166	9051	9053	-	-	-
Hydroelectric	44.92	8	10	63	108	119	125	138
		143	152	153	156	170	176	177
		185	186	187	191	213	230	233
		238	7001	7002	7017	7023	7024	7049
		7055	7071	9002	-	-	-	-
Wind	5.80	91	146	242	7044	-	-	-
Photovoltaic	2.90	9054	9055	-	-	-	-	-

Neighborhood Structure N₂

This neighborhood structure adds the constraints (26)-(29) to the complete relaxed deterministic AC-OPF model and relaxes $n_{ij,s}^{t}$ and $n_{i,s}^{sh}$ as in N_1.

$$\ddot{n}_{ij,s}^{t} \le n_{ij,s}^{t} \le \ddot{n}_{ij,s}^{t} + k_{tp} \qquad \forall (ij \in \Gamma_T, s \in \Gamma_S) \tag{26}$$

$$\ddot{n}_{i,s}^{sh} \le n_{i,s}^{sh} \le \ddot{n}_{i,s}^{sh} + k_{sh} \qquad \forall (i \in \Gamma_{SH}, s \in \Gamma_S) \tag{27}$$

$$\sum_{\Omega_T} \ddot{n}_{ij,s}^{t} \le \sum_{\Omega_T} n_{ij,s}^{t} \le k_{tp} + \sum_{\Omega_T} \ddot{n}_{ij,s}^{t} \tag{28}$$

$$\sum_{\Omega_{BC}} \ddot{n}_{i,s}^{sh} \le \sum_{\Omega_{BC}} n_{i,s}^{sh} \le k_{sh} + \sum_{\Omega_{BC}} \ddot{n}_{i,s}^{sh} \tag{29}$$

These constraints only allow an increase in the current position of a single OLTC and a single controllable shunt compensator. In this way, the value of a single $n_{ij,s}^{t}$ and a single $n_{i,s}^{sh}$ can be increased in k_{tp} and k_{sh} steps, respectively. This structure does not obligate changes in the variables, so it is possible to preserve the current position in order to maintain the optimality.

Neighborhood Structure N₃

This neighborhood structure follows the same conception of neighborhood structure N_2. In this regard, the integrality constraints of variables $n_{ij,s}^{t}$ and $n_{i,s}^{sh}$ are relaxed to add constraints (30)–(33) to the AC-OPF model.

$$\ddot{n}_{ij,s}^{t} - k_{tp} \le n_{ij,s}^{t} \le \ddot{n}_{ij,s}^{t} \qquad \forall (km \in \Gamma_T, s \in \Gamma_S) \tag{30}$$

$$\ddot{n}_{i,s}^{sh} - k_{sh} \le n_{i,s}^{sh} \le \ddot{n}_{i,s}^{sh} \qquad \forall (k \in \Gamma_{SH}, s \in \Gamma_S) \tag{31}$$

$$k_{tp} - \sum_{\Omega_T} \ddot{n}_{ij,s}^{t} \le \sum_{\Omega_T} n_{ij,s}^{t} \le \sum_{\Omega_T} \ddot{n}_{ij,s}^{t} \tag{32}$$

$$k_{sh} - \sum_{\Omega_{BC}} \ddot{n}_{i,s}^{sh} \le \sum_{\Omega_{BC}} n_{i,s}^{sh} \le \sum_{\Omega_{BC}} \ddot{n}_{i,s}^{sh} \tag{33}$$

This structure allows decreasing the current position of the tap of a single OLTC and the current modules state of a single shunt compensator. So, the value of $n_{ij,s}^{t}$ and $n_{i,s}^{sh}$ will decrease in k_{tp} and k_{sh} steps just for one OLTC and one shunt compensator, respectively. Like previous structures, N_3 does not force the decrease in a variable when it is not necessary. In the simulated tests, the values for parameters were $k_{tp} = 2$ and $k_{sh} = 1$.

It is important mentioning that the above structures can be implemented in any sequence to obtain a good performance. In this regard, based on empirical evidence, we choose the sequence N_1, N_2, and N_3 to solve the problem. Thus, at the beginning of the iterative process, the structure N_1 diversifies the exploration process allowing two directions (increasing or decreasing tap steps). When there is no possibility of improving the objective function, the following structure N_2 is applied for search in one direction (increasing tap steps). Note that parameters k_{tp} and k_{sh} should change since there are no improving moves for those values (reason to change the first structure). In the same way, the iterative process continues until it is not possible to improve the current solution of the algorithm, then the structure N_3 is applied. For this last structure, the direction of exploration changes, and the value for the parameters may vary or not. In conclusion, changing the search structures need a variation in parameters k_{tp} and k_{sh}.

3) Proposed Algorithm:

The methodology to solve the proposed AC-OPF model consists of finding an initial solution considering the AC-OPF model, followed by the initialization of the VND matheuristic algorithm.

The flowchart in Fig. *2* illustrates the structure of the VND matheuristic algorithm to solve the probabilistic AC-OPF problem. Where Pr represents the Pareto set of solutions, ψ represents the current value of all discrete variables $\ddot{n}_{i,s}^{sh}$ and $\ddot{n}_{ij,s}^{t}$ (taps of OLTCs and shunt (compensators) of the problem, $f(\psi)$ represents the value of objective function considering ψ as input parameter, γ represents a candidate solution for the problem (objective function and integer variables values), ψ' represents the neighbor solution of ψ (integer values) and K is the number of neighborhood structures considered.

For each weight value, the execution of the VND algorithm ends when the search process carried out over the set of neighborhood structures is explored, and no improvement in the current solution is obtained. Finally, the process gives the Pareto frontier of the problem.

IV. TEST AND RESULTS

The proposed methodology is tested and analyzed by adopting the IEEE 300-bus system "*pglib_opf_case300_ieee system*" v.19.5 [38]. The MINLP model and the VND algorithm

TABLE III
RESULTS FOR THE POPF FOR CASES 1 AND 2 – LOAD SCENARIO 1

ω	Case 1 Generation cost [MUS$]	Emission [kt CO_2 eq.]	CPU Time [s]	Relaxed OPF (#)	Fixed OPF (#)	Case 2 Generation cost [MUS$]	Emission [kt CO_2 eq.]	CPU Time [s]	Relaxed OPF (#)	Fixed OPF (#)
1.0	362.39	165.46	29.50	16	51	351.83	32.18	69.69	21	330
0.9	337.84	169.05	88.98	21	66	352.40	29.57	18.78	5	90
0.8	381.48	124.51	5.20	6	21	366.75	14.60	32.88	8	135
0.7	456.40	77.40	4.61	5	18	378.02	7.49	16.95	5	90
0.6	505.28	58.97	6.50	5	18	384.64	4.97	27.50	5	90
0.5	551.25	47.60	12.98	6	21	388.94	3.89	77.16	10	165
0.4	588.95	41.40	30.09	9	30	392.35	3.32	21.08	5	90
0.3	628.16	37.15	30.67	8	27	395.42	2.99	100.70	17	270
0.2	665.40	34.64	20.17	5	18	398.86	2.76	63.88	14	225
0.1	712.03	33.09	20.02	5	18	405.58	2.54	49.19	16	255
0.0	789.13	32.23	26.42	5	18	469.81	2.28	21.48	12	195
Total			**275.16**	**91**	**306**	**Total**		**499.28**	**118**	**1935**

TABLE IV
RESULTS FOR THE POPF FOR CASES 1 AND 2 – LOAD SCENARIO 2

ω	Case 1 Generation cost [MUS$]	Emission [kt CO_2 eq.]	CPU Time [s]	Relaxed OPF (#)	Fixed OPF (#)	Case 2 Generation cost [MUS$]	Emission [kt CO_2 eq.]	CPU Time [s]	Relaxed OPF (#)	Fixed OPF (#)
1.0	2204.50	610.84	6.81	6	21	1996.92	140.73	29.70	9	150
0.9	2213.66	577.85	9.53	12	39	2001.30	120.91	49.42	18	285
0.8	2252.16	536.61	4.80	6	21	2035.63	86.52	33.36	12	195
0.7	2525.05	371.52	21.16	28	87	2080.62	58.27	45.30	17	270
0.6	2728.42	293.70	7.59	9	30	2114.91	45.29	53.48	19	300
0.5	2885.13	255.01	11.48	14	45	2148.96	36.79	66.09	23	360
0.4	3037.37	229.80	8.47	10	33	2180.84	31.48	69.69	25	390
0.3	3156.17	216.82	7.28	8	27	2215.35	27.72	26.44	9	150
0.2	3267.79	209.53	8.63	10	33	2259.53	24.77	15.44	5	90
0.1	3492.46	201.68	4.52	5	18	2317.70	22.76	15.53	5	90
0.0	3641.55	199.86	4.58	5	18	2441.70	21.39	65.73	23	360
Total			**94.84**	**113**	**372**	**Total**		**470.19**	**165**	**2640**

TABLE V
RESULTS FOR THE POPF FOR CASES 1 AND 2 – LOAD SCENARIO 3

ω	Case 1 Generation cost [MUS$]	Emission [kt CO_2 eq.]	CPU Time [s]	Relaxed OPF (#)	Fixed OPF (#)	Case 2 Generation cost [MUS$]	Emission [kt CO_2 eq.]	CPU Time [s]	Relaxed OPF (#)	Fixed OPF (#)
1.0	571.95	114.97	47.31	31	96	508.06	31.58	40.27	11	180
0.9	571.39	111.07	24.88	11	36	508.19	29.50	57.03	14	225
0.8	575.48	105.90	42.31	17	54	509.54	27.91	51.83	11	180
0.7	602.52	90.37	16.88	7	24	517.68	23.12	26.27	5	90
0.6	632.68	78.91	20.03	11	36	526.70	19.74	21.19	5	90
0.5	657.56	72.76	14.30	8	27	535.18	17.62	57.22	15	240
0.4	677.37	69.46	11.77	7	24	543.05	16.33	77.31	18	285
0.3	691.01	67.97	8.42	5	18	551.28	15.45	33.58	8	135
0.2	713.57	66.53	8.02	5	18	559.61	14.89	23.73	5	90
0.1	745.19	65.37	8.58	5	18	576.19	14.25	64.66	10	165
0.0	761.28	65.19	8.86	5	18	591.20	14.08	27.42	5	90
Total			**211.34**	**112**	**369**	**Total**		**480.50**	**107**	**1770**

were implemented in AMPL [39] and solved with the solver KNITRO with default settings, using a computer with an Intel i7-6700 @ 3.4GHz processor and 8GB of RAM.

The carried-out tests aim to show the performance of the proposed MA considering the simultaneous optimization of the two objective functions. In the tests, two different cases are considered to validate the proposed methodology:

- **Case 1:** The electrical system has thermal generators only.
- **Case 2:** The system has polluting thermal, hydraulic, wind, and photovoltaic generation sources.

In both cases, a planning horizon of one year with three load scenarios is considered. Table I presents the probabilistic load parameters (mean (μ) and standard deviation (σ)) and operation period time during a year in each scenario [41]. In all tests, the AC-OPF problem was solved considering weight steps $\Delta\omega$ = 0.1, then, the weights ω = [0, 0.1, 0.2, … ,1] for the convex combination of two objective functions generating eleven non-dominated solutions

Table I presents the means and standard deviations of the probability density functions adopted for RES (wind and photovoltaic). For the wind speed curve, the skewness and kurtosis values are 0.638 and 3.364, respectively, in all the load scenarios.

TABLE VII
ACTIVE AND REACTIVE POWER INJECTED BY THERMAL GENERATORS FOR CASE 1 AND 2 - LOAD SCENARIO 1

	Case 1			Case 2		
ω	P^T Total [MW]	P^{RES} Total [MW]	Shunt Total [MVAr]	P^T Total [MW]	P^{RES} Total [MW]	Shunt [MVAr]
1.0	12162.60	0.00	-426.04	2637.48	9419.54	-426.69
0.9	12152.44	0.00	-474.90	2326.30	9731.7	-426.69
0.8	12051.92	0.00	-474.90	1689.06	10375.24	-437.94
0.7	12000.72	0.00	-474.90	1226.28	10853.64	19.60
0.6	11974.42	0.00	-474.90	987.99	11103.78	-437.94
0.5	11951.64	0.00	-474.90	837.78	11263.85	-499.57
0.4	11941.07	0.00	-474.90	759.87	11345.76	-499.57
0.3	11935.34	0.00	-474.90	727.44	11382.19	-464.57
0.2	11934.41	0.00	-474.90	756.05	11353.2	-438.90
0.1	11939.74	0.00	-474.90	918.42	11180.05	-419.48
0.0	11950.29	0.00	-474.90	1428.67	10651.68	-419.48

TABLE VIII
ACTIVE AND REACTIVE POWER INJECTED BY THERMAL GENERATORS FOR CASE 1 AND 2 - LOAD SCENARIO 2

	Case 1			Case 2		
ω	P^T Total [MW]	P^{RES} Total [MW]	Shunt Total [MVAr]	P^T Total [MW]	P^{RES} Total [MW]	Shunt [MVAr]
1.0	19329.90	0.00	-254.83	5235.65	14073.72	-254.09
0.9	19280.96	0.00	-243.44	4881.96	14435.35	-204.91
0.8	19219.81	0.00	-243.44	4575.27	14747.68	-253.81
0.7	19153.35	0.00	-500.66	4366.88	14955.04	31.31
0.6	19145.81	0.00	-500.66	4322.52	14984.52	-228.06
0.5	19133.00	0.00	-527.16	4311.60	14995.4	-263.06
0.4	19124.81	0.00	-527.16	4301.61	15004.45	-133.68
0.3	19125.56	0.00	-527.16	4300.41	15004.22	-125.06
0.2	19130.82	0.00	-527.16	4320.18	14995.35	-125.06
0.1	19142.10	0.00	-527.16	4361.73	14972.06	-125.06
0.0	19154.58	0.00	-527.16	4526.40	14842.53	-221.93

TABLE IX
ACTIVE AND REACTIVE POWER INJECTED BY THERMAL GENERATORS FOR CASE 1 AND 2 - LOAD SCENARIO 3

	Case 1			Case 2		
ω	P^T Total [MW]	P^{RES} Total [MW]	Shunt Total [MVAr]	P^T Total [MW]	P^{RES} Total [MW]	Shunt [MVAr]
1.0	24050.96	0.00	115.22	9151.69	14901.49	59.34
0.9	24029.43	0.00	62.22	9119.40	14942.53	-68.66
0.8	23998.85	0.00	17.41	9103.72	14946.16	-94.41
0.7	23972.83	0.00	17.41	9076.66	14954.26	39.65
0.6	23964.58	0.00	17.41	9069.23	14955.29	-94.41
0.5	23956.11	0.00	17.41	9053.72	14954.05	-122.66
0.4	23948.85	0.00	17.41	9054.56	14947.94	-122.66
0.3	23945.25	0.00	17.41	9055.04	14942.31	-122.66
0.2	23941.11	0.00	17.41	9063.34	14937.65	-122.66
0.1	23945.40	0.00	17.41	9066.44	14938.49	-123.25
0.0	23946.63	0.00	17.41	9083.26	14934.29	-123.25

The *pglib_opf_case300_ieee* system is tested to assess the scalability of the proposed methodology in a large-scale system. This system consists of 300 buses, 69 generating units, 411 transmission lines, 129 transformers with the variable tap, and 14 bars with variable reactive banks. The values of voltage magnitudes of the buses must be in the range of 0.94 to 1.06 *per unit*. For Case 2, the generation technologies installed in the system buses are presented in Table II.

In this section, Table III, Table IV, and Table V show the generation costs and the volume of GHG emissions, the processing time, and the number of relaxed and fixed AC-OPF calculations for all load scenarios in both cases, respectively. Fig. *3*, Fig. *4*, and Fig. *5* show the graphs of the Pareto solution curves for each considered load scenario in Case 1 and Case 2 that were obtained by the proposed methodology. Finally, Tables VI-VIII present the total active power generated by thermal and RES generation units, and the reactive power injected by shunt compensators in the system.

V. DISCUSSION

Before starting to analyze the solutions obtained, it is important to know that all *a priori* method solutions are optimal individually. However, all solutions must be analyzed to find the most appropriate solution from the point of view of the decision maker, which should adopt it as a final solution [40]. The uncertainties used in this research are based on others studies and assess the effectiveness of the approach developed [29], [41].

TABLE VI
PERCENTAGE REDUCTION BETWEEN CASES 1 AND 2

	Load scenario 1		Load scenario 2		Load scenario 3	
ω	Generation cost (%)	Emission (%)	Generation cost (%)	Emission (%)	Generation cost (%)	Emission (%)
1.0	2.91	80.55	9.42	76.96	11.17	72.53
0.9*	-4.31	82.51	9.59	79.08	11.06	73.44
0.8	3.86	88.27	9.61	83.88	11.46	73.65
0.7	17.17	90.32	17.60	84.32	14.08	74.42
0.6	23.88	91.58	22.49	84.58	16.75	74.98
0.5	29.45	91.83	25.52	85.57	18.61	75.78
0.4	33.38	91.97	28.20	86.30	19.83	76.48
0.3	37.05	91.95	29.81	87.21	20.22	77.28
0.2	40.06	92.03	30.85	88.18	21.58	77.61
0.1	43.04	92.33	33.64	88.71	22.68	78.20
0.0	40.47	92.91	32.95	89.30	22.34	78.40

Comparing the results presented in Fig. *3*, Fig. *4*, and Fig. *5* for all the 11 analyzed weights, considering a power system with polluting thermal, hydraulic, wind, and photovoltaic generation (Case 2), better results were obtained, both to minimize the generation cost as to reduce the GHG emissions. For generation costs, considering the case that there are RESs, the methodology provides solutions in which costs are reduced by an average of 21.40%, due to lower operating cost of the RES, in addition to simultaneously and substantially reducing GHG emissions on average 83.43 Table IX shows the percentages of reduction in the values of objectives functions of Case 2 in relation to Case 1. The highlighted value in Table VI is the single weighting of the objective functions where the solution of Case 1 presents a better result than Case 2; this result is associated with the weight ω = 0.9 of load scenario 1. Due to non-convexity of the OPF model, this solution is dominated by the solutions obtained with the other weights; this aspect is illustrated in Fig. *3*.

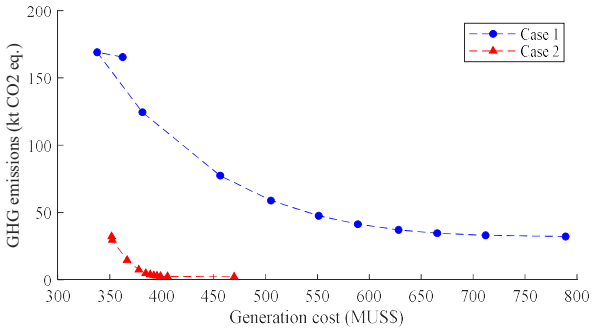

Fig. 3. Pareto curves – Load scenario 1

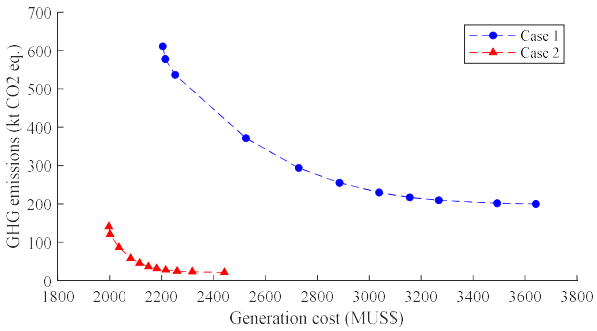

Fig. 4. Pareto curves– Load scenario 2

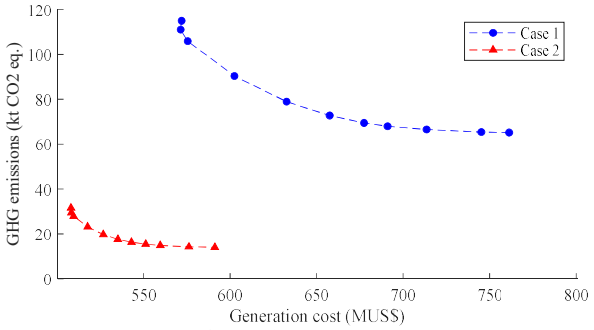

Fig. 5. Pareto curves – Load scenario 3

Tables VII – VIII, show the power injection differences between case 1 and case 2. Results present a significant reduction in the active power injection of thermal units from case 1 to case 2, it is expected due to the high penetration of RES in the system. The mean reduction of total thermal generation is 89.2%, 76.5%, and 62.1% for load scenarios 1, 2, and 3, respectively.

In case 2 and low-load scenario 1, the mean active power generated by thermal units varies from 6% to 21.9% of the total active power of the system. On the other hand, for load scenarios 2 and 3, the RES generation reach higher levels near to the generation limits presenting similar behaviors. In this regard, the mean active power generated by thermal units represent 23.3% and 37.8% of the total active power generation of the system, for load scenarios 2 and 3, respectively.

Obtained solutions are all feasible and voltage profile and shun injection and tap positions present different behavior for

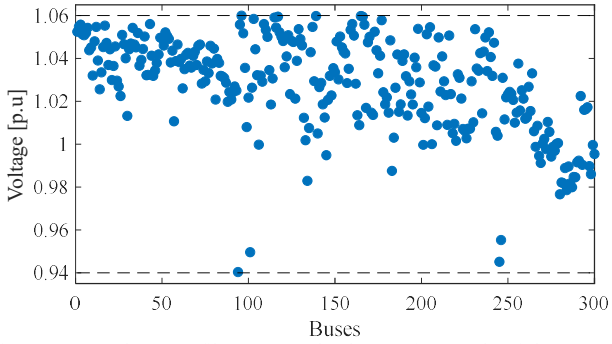

Fig. 6. Mean voltage profile – Case 1, load scenario 1, and weight = 1.0

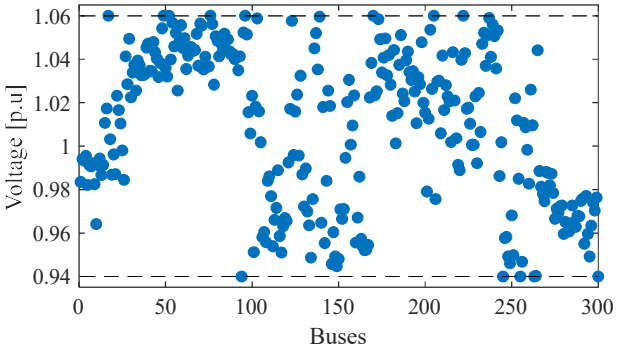

Fig 7. Mean voltage profile – Case 1, load scenario 1 and weight = 0.0

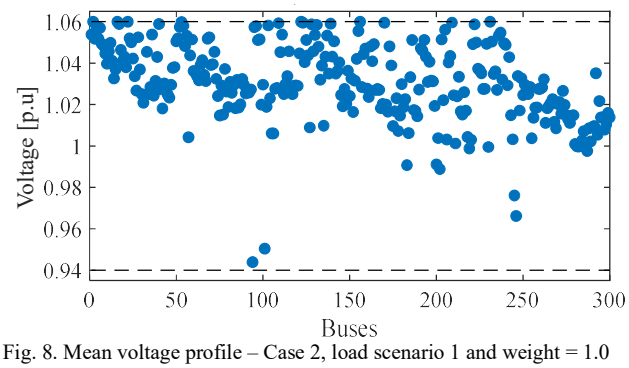

Fig. 8. Mean voltage profile – Case 2, load scenario 1 and weight = 1.0

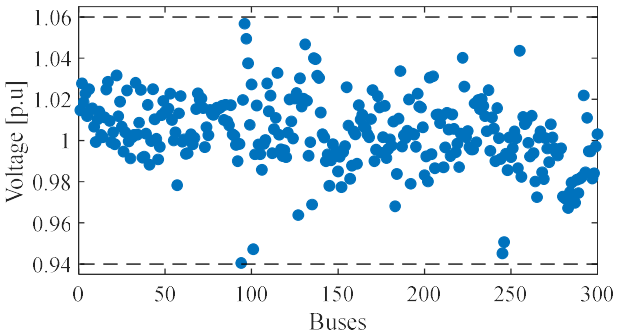

Fig. 9 Mean voltage profile – Case 2, load scenario 1 and weight = 0.0

all cases. Simulations reveal that, the mean voltage profile of the system escalates near the upper voltage limit while the weight parameter increases giving priority to objective function f^A that minimizes the fuel generation costs. An example of this behavior is presented in Fig. 6 – Fig. 9. Complete results are available in [42], including voltage profiles, tap positions of the

transformer, and shunt compensators for each study case and load scenario.

Related to the number of AC-OPF that were calculated and the processing time, in Case 2, an average of 1.23 and 6.06 times more AC-OPF were executed with the relaxed model and the proposed model, respectively, considering the discrete variables the taps of the transformers and the fixed shunt compensator, and the processing time was on average 2.69 times longer than for Case 1.

VI. Conclusion

The obtained results allow us to conclude that the proposed algorithm is efficient and presents a good performance in terms of computational time and robustness for the solution of the AC-OPF problem with discrete, stochastic, and multiobjective characteristics; it can provide a set of Pareto solutions. The proposed matheuristic approach provides good quality solutions with low computational time; it is promising for solving planning and operating problems in large-scale electric power systems. Results show that the multiobjective approach is the most adequate to address the AC-OPF problem because the emissions of greenhouse gases can be controlled through the redesign of the generating parks, directly interfering with the system's generation costs. Renewable energy sources are adequate to face climate challenges, however, the availability of their primary energy sources is uncertain, so they must be supported by dispatchable generation.

Future works could adopt the presence of energy storage devices and explore different matheuristic approaches.

References

[1] H. Dommel and W. Tinney, "Optimal power flow solutions," *IEEE Trans. Power Appar. Syst.*, vol. PAS-87, no. 10, pp. 1866–1876, Oct. 1968, doi: 10.1109/TPAS.1968.292150.

[2] J. CARPENTIER, "Optimal power flows," *Int. J. Electr. Power Energy Syst.*, vol. 1, no. 1, pp. 3–15, Apr. 1979, doi: 10.1016/0142-0615(79)90026-7.

[3] A. Gómez-Expósito, A. J. Conejo, and C. Cañizares, *Electric energy systems: Analysis and operation*, vol. 17. CRC Press, 2017.

[4] A. A. El-Keib, H. Ma, and J. L. Hart, "Economic dispatch in view of the Clean Air Act of 1990," *IEEE Trans. Power Syst.*, vol. 9, no. 2, pp. 972–978, May 1994, doi: 10.1109/59.317648.

[5] M. A. Abido, "A new multiobjective evolutionary algorithm for environmental/economic power dispatch," in *Proceedings of the IEEE Power Engineering Society Transmission and Distribution Conference*, 2001, vol. 2, no. SUMMER, pp. 1263–1268, doi: 10.1109/pess.2001.970254.

[6] M. A. Abido, "Environmental/Economic Power Dispatch Using Multiobjective Evolutionary Algorithms," *IEEE Trans. Power Syst.*, vol. 18, no. 4, pp. 1529–1537, 2003, doi: 10.1109/TPWRS.2003.818693.

[7] US Dept. of State, "Leaders Summit on Climate - United States Department of State," *The White House*, 2021. https://www.whitehouse.gov/briefing-room/statements-releases/2021/04/23/leaders-summit-on-climate-summary-of-proceedings/ (accessed Jun. 10, 2021).

[8] B. Mather and G. Yuan, "Onward and Upward: Distributed Energy Resource Integration," *IEEE Power Energy Mag.*, vol. 18, no. 6, Nov. 2020, doi: 10.1109/MPE.2020.3016100.

[9] F. P. Mahdi, P. Vasant, V. Kallimani, J. Watada, P. Y. S. Fai, and M. Abdullah-Al-Wadud, "A holistic review on optimization strategies for combined economic emission dispatch problem," *Renewable and Sustainable Energy Reviews*, vol. 81. Elsevier Ltd, pp. 3006–3020, Jan. 2018, doi: 10.1016/j.rser.2017.06.111.

[10] M. A. Ilyas, G. Abbas, T. Alquthami, M. Awais, and M. B. Rasheed, "Multiobjective optimal power flow with integration of renewable energy sources using fuzzy membership function," *IEEE Access*, vol. 8, pp. 143185–143200, 2020, doi: 10.1109/ACCESS.2020.3014046.

[11] A. Maulik and D. Das, "Optimal power dispatch considering load and renewable generation uncertainties in an AC–DC hybrid microgrid," *IET Gener. Transm. Distrib.*, vol. 13, no. 7, pp. 1164–1176, Apr. 2019, doi: 10.1049/iet-gtd.2018.6502.

[12] M. A. Abido, "Multiobjective evolutionary algorithms for electric power dispatch problem," *IEEE Trans. Evol. Comput.*, vol. 10, no. 3, pp. 315–329, Jun. 2006, doi: 10.1109/TEVC.2005.857073.

[13] M. A. Abido, "Multiobjective particle swarm optimization for environmental/economic dispatch problem," *Electr. Power Syst. Res.*, vol. 79, no. 7, pp. 1105–1113, 2009, doi: 10.1016/j.epsr.2009.02.005.

[14] L. H. Wu, Y. N. Wang, X. F. Yuan, and S. W. Zhou, "Environmental/economic power dispatch problem using multiobjective differential evolution algorithm," *Electr. Power Syst. Res.*, vol. 80, no. 9, pp. 1171–1181, Sep. 2010, doi: 10.1016/j.epsr.2010.03.010.

[15] F. Chen, G. H. Huang, Y. R. Fan, and R. F. Liao, "A nonlinear fractional programming approach for environmental-economic power dispatch," *Int. J. Electr. Power Energy Syst.*, vol. 78, pp. 463–469, 2016, doi: 10.1016/j.ijepes.2015.11.118.

[16] S. Sivasubramani and K. S. Swarup, "Environmental/economic dispatch using multiobjective harmony search algorithm," *Electr. Power Syst. Res.*, vol. 81, no. 9, pp. 1778–1785, Sep. 2011, doi: 10.1016/j.epsr.2011.04.007.

[17] D. Aydin, S. Özyön, C. Yaşar, and T. Liao, "Artificial bee colony algorithm with dynamic population size to combined economic and emission dispatch problem," *Int. J. Electr. Power Energy Syst.*, vol. 54, pp. 144–153, 2014, doi: 10.1016/j.ijepes.2013.06.020.

[18] M. Modiri-Delshad and N. A. Rahim, "Multiobjective backtracking search algorithm for economic emission dispatch problem," *Appl. Soft Comput. J.*, vol. 40, pp. 479–494, Mar. 2016, doi: 10.1016/j.asoc.2015.11.020.

[19] V. K. Jadoun, N. Gupta, K. R. Niazi, and A. Swarnkar, "Modulated particle swarm optimization for economic emission dispatch," *Int. J. Electr. Power Energy Syst.*, vol. 73, pp. 80–88, Dec. 2015, doi: 10.1016/j.ijepes.2015.04.004.

[20] A. Y. Abdelaziz, E. S. Ali, and S. M. Abd Elazim, "Combined economic and emission dispatch solution using Flower Pollination Algorithm," *Int. J. Electr. Power Energy Syst.*, vol. 80, pp. 264–274, Sep. 2016, doi: 10.1016/j.ijepes.2015.11.093.

[21] Y. A. Gherbi, H. Bouzeboudja, and F. Z. Gherbi, "The combined economic environmental dispatch using new hybrid metaheuristic," *Energy*, vol. 115, pp. 468–477, Nov. 2016, doi: 10.1016/j.energy.2016.08.079.

[22] Y. A. Gherbi, F. Lakdja, H. Bouzeboudja, and F. Z. Gherbi, "Hybridization of two metaheuristics for solving the combined economic and emission dispatch problem," *Neural Comput. Appl.*, vol. 31, no. 12, pp. 8547–8559, Dec. 2019, doi: 10.1007/s00521-019-04151-7.

[23] R. Dong and S. Wang, "New optimization algorithm inspired by kernel tricks for the economic emission dispatch problem with valve point," *IEEE Access*, vol. 8, pp. 16584–16594, 2020, doi: 10.1109/ACCESS.2020.2965725.

[24] A. Chatterjee, S. P. Ghoshal, and V. Mukherjee, "Solution of combined economic and emission dispatch problems of power systems by an opposition-based harmony search algorithm," *Int. J. Electr. Power Energy Syst.*, vol. 39, no. 1, pp. 9–20, Jul. 2012,

doi: 10.1016/j.ijepes.2011.12.004.
[25] S. Jiang, Z. Ji, and Y. Shen, "A novel hybrid particle swarm optimization and gravitational search algorithm for solving economic emission load dispatch problems with various practical constraints," *Int. J. Electr. Power Energy Syst.*, vol. 55, pp. 628–644, 2014, doi: 10.1016/j.ijepes.2013.10.006.
[26] L. R. Robert and L. R. S. Ravi Singh, "Economic emission dispatch of hydro-thermal-wind using CMQLSPSN technique," *IET Renew. Power Gener.*, Jul. 2020, doi: 10.1049/iet-rpg.2019.1232.
[27] S. K. Damodaran and T. K. S. Kumar, "Hydro-thermal-wind generation scheduling considering economic and environmental factors using heuristic algorithms," *Energies*, vol. 11, no. 2, Feb. 2018, doi: 10.3390/en11020353.
[28] C. Li, W. Wang, and D. Chen, "Multiobjective complementary scheduling of hydro-thermal-RE power system via a multiobjective hybrid grey wolf optimizer," *Energy*, vol. 171, pp. 241–255, Mar. 2019, doi: 10.1016/j.energy.2018.12.213.
[29] E. X. S. Araujo, M. C. Cerbantes, and J. R. S. Mantovani, "Optimal power flow with renewable generation: a modified NSGA-II-based probabilistic solution approach," *J. Control. Autom. Electr. Syst.*, no. March 2015, May 2020, doi: 10.1007/s40313-020-00596-7.
[30] S. Montoya-Bueno, J. I. Munoz, and J. Contreras, "A Stochastic Investment Model for Renewable Generation in Distribution Systems," *IEEE Trans. Sustain. Energy*, vol. 6, no. 4, pp. 1466–1474, Oct. 2015, doi: 10.1109/TSTE.2015.2444438.
[31] J. M. Home-Ortiz, W. C. De Oliveira, and J. R. S. Mantovani, "Optimal power flow problem solution through a matheuristic approach," *IEEE Access*, vol. 9, pp. 84576–84587, 2021, doi: 10.1109/ACCESS.2021.3087626.
[32] B. Borkowska, "Probabilistic Load Flow," *IEEE Trans. Power Appar. Syst.*, vol. PAS-93, no. 3, pp. 752–759, May 1974, doi: 10.1109/TPAS.1974.293973.
[33] Z. Wang and F. L. Alvarado, "Interval arithmetic in power flow analysis," *IEEE Trans. Power Syst.*, vol. 7, no. 3, pp. 1341–1349, 1992, doi: 10.1109/59.207353.
[34] J. M. Morales and J. Perez-Ruiz, "Point Estimate Schemes to Solve the Probabilistic Power Flow," *IEEE Trans. Power Syst.*, vol. 22, no. 4, pp. 1594–1601, Nov. 2007, doi: 10.1109/TPWRS.2007.907515.
[35] G. Verbic, a Claudio, and a Canizares, "Probabilistic optimal power flow in electricity markets based on a two point estimate method," *IEEE Trans. Power Syst.*, vol. 21, no. 4, pp. 1883–1894, 2006.
[36] H. P. Hong, "An efficient point estimate method for probabilistic analysis," *Reliab. Eng. Syst. Saf.*, vol. 59, no. 3, pp. 261–267, Mar. 1998, doi: 10.1016/S0951-8320(97)00071-9.
[37] R. T. Sataloff, M. M. Johns, and K. M. Kost, *Matheuristics Hybridizing Metaheuristics and Mathematical Programming*, vol. 10. Boston, MA: Springer US, 2010.
[38] S. Babaeinejadsarookolaee *et al.*, "The power grid library for benchmarking ac optimal power flow algorithms," *arXiv*, pp. 1–17, Aug. 2019, [Online]. Available: http://arxiv.org/abs/1908.02788.
[39] R. Fourer, D. M. Gay, and B. W. Kernighan, *A modeling language for mathematical programming*. 1990.
[40] J. Branke, K. Miettinen, K. Deb, and R. Słowi'nski, *Multiobjective optimization: interactive and evolutionary approaches*, vol. 5252 LNCS. Springer-Verlag Berlin Heidelberg, 2008.
[41] B. R Pereira, G. R. D. C Martins, J. Contreras J. R. S. Mantovani, "Optimal distributed generation and reactive power allocation in electrical distribution systems," *IEEE Trans. Sustain. Energy*, v. 7, n. 3, 2016, doi: 10.1109/TSTE.2015.2512819
[42] LaPSEE Power System Test Cases Repository https://www.feis.unesp.br/#!/departamentos/engenharia-eletrica/pesquisas-e-projetos/lapsee/downloads/materiais-de-cursos1193/

Wmerson Claro de Oliveira received a B.Sc. degree in electrical engineering from the Universidade do Estado de Mato Grosso (UNEMAT), Brazil, in 2018 and an M.Sc degree in electrical engineering from the São Paulo State University (UNESP), Ilha Solteira, Brazil, in 2020. His research interests include the development of methodologies for the optimization of electrical power systems.

Jairo Gonzalo Yumbla Romero received the B.Sc. degree from the University of Cuenca, Cuenca, Ecuador, in 2018, and the M.Sc. degree from the São Paulo State University (UNESP), Ilha Solteira, Brazil, in 2021; both in electrical engineering. He is currently pursuing his doctor's degree at the UNESP. His research interests include the development of methodologies for the planning and control of electrical power systems, renewable energies, and applications of artificial intelligence for smart grids.

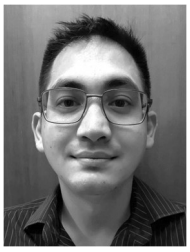

Lucas do Carmo Yamaguti received B.Sc. and M.Sc. degrees from the Sao Paulo State University (UNESP), Ilha Solteira, Brazil, in 2017 and 2019, respectively, all in electrical engineering. He is currently working for a Ph.D. degree at the Sao Paulo State University (UNESP), Ilha Solteira, Brazil. His research interests include the development of methodologies for the optimization and planning of electrical power systems.

Juan M. Home-Ortiz received the B.Sc. and M.Sc. degrees in electrical engineering from the Universidad Tecnológica de Pereira, Colombia, in 2011 and 2014, respectively, and the Ph.D. degree in electrical engineering from the São Paulo State University (UNESP), Ilha Solteira, Brazil, in 2019. Currently, he is carrying out postdoctoral research with the UNESP. His research interests include the development of methodologies for the optimization, planning, and control, of electrical power systems.

José Roberto Sanches Mantovani (M'06) received the B.Sc. degree from the Sao Paulo State University (UNESP), Ilha Solteira, Brazil, in 1981, and the M.Sc. and Ph.D. degrees from the University of Campinas, Campinas, Brazil, in 1987 and 1995, respectively, all in electrical engineering. He is currently a Professor with the Department of Electrical Engineering, UNESP. His research interests include the development of methodologies for the optimization, planning, and control of electrical power systems and applications of artificial intelligence in power systems.